Ag/6*H*-SiC(0001) surface phase and its structural transformation upon exposure to atomic hydrogen

O. Kubo,[1,*] J. T. Ryu,[1,2] M. Katayama,[1,†] and K. Oura[1]
[1]*Department of Electronic Engineering, Graduate School of Engineering, Osaka University, 2-1 Yamadaoka, Suita, Osaka 565-0871, Japan*
[2]*Department of Computer and Communication Engineering, Taegu University, 15 Naeri, Jinryang, Kyungsan, Kyungpook 712-714, Korea*
(Received 24 February 2003; revised manuscript received 26 June 2003; published 15 January 2004)

The surface phase of Ag/6*H*-SiC(0001) and its structural transformation upon exposure to atomic hydrogen were investigated using scanning tunneling microscopy (STM). Ag deposition onto the 6*H*-SiC(0001)$\sqrt{3}\times\sqrt{3}$ surface at 500 °C resulted in the formation of a 3×3-Ag structure that coexisted with a homogeneous two-dimensional (2D) Ag layer without showing any periodicities. The scanning tunneling spectroscopy spectrum of a 2D Ag layer exhibited metallic behavior. After atomic hydrogen exposure at 300 °C, the 2D Ag layer changed into 3D Ag clusters, while the 3×3-Ag area became disordered, exhibiting only a few Ag clusters. The 3×3-Ag area and the 2D Ag layer were reproduced by annealing at 500 °C. This result is similar to atomic-hydrogen-induced self-organization processes on Si substrates covered with a monatomic metal layer.

DOI: 10.1103/PhysRevB.69.045406 PACS number(s): 68.35.Bs, 68.35.Fx, 68.43.Hn, 68.55.Jk

I. INTRODUCTION

Silicon carbide (SiC) has attracted attention for application to high-power and high-frequency devices because of its high thermal conductivity, high breakdown field, and wide band gap. Among many polytypes of SiC, the 4*H* and 6*H* polytypes are suitable for various applications and have been studied extensively.[1–5] Recently, the Schottky diode made of SiC epitaxial layers has been demonstrated successfully,[6] and the use of SiC as a substrate in the heteroepitaxial growth of group III nitrides is anticipated.[7] With regard to these applications, in-depth elucidation of surface properties of SiC is of great importance and indeed they have been well investigated in recent years.[8] Adsorption of metals onto SiC substrate has also been investigated for Al, Co, and Ti adsorbates.[7,9,10] While it is well known that metal adsorption on Si surfaces results in the formation of various reconstructed two-dimensional (2D) layers,[11] only the formation of metal clusters or three-dimensional (3D) islands with no reconstruction has been reported for SiC substrates.

Recently, several works have been reported concerning the interaction of atomic hydrogen (H) with metal-induced Si surface phases,[12] in which the substitutional adsorption of H atoms causes the formation of metal clusters of nanometer size. This phenomenon can be regarded as a self-organization process from the 2D structure of an adsorbate layer to 3D islands, which is triggered by adsorption of H. For typical systems such as Ag/Si(111) (Ref. 13) and In/Si(100),[14,15] the correlation between the H-induced cluster formation process and the original surface structure has been investigated. However, such H-induced self-organization has only been studied in metal/Si systems.

In this study, we have investigated the surface phase of Ag/6*H*-SiC(0001) and its structural transformation process upon atomic hydrogen exposure using scanning tunneling microscopy (STM). After deposition of Ag on the 6*H*-SiC(0001)$\sqrt{3}\times\sqrt{3}$ surface at 500 °C, a 3×3 periodic surface phase was found, which was different from the clean SiC(0001)3×3 surface. The 3×3 periodic surface always coexisted with a homogeneous 2D Ag layer without showing any periodicities. The scanning tunneling spectroscopy (STS) spectrum of the 2D Ag layer exhibited metallic behavior. When this surface was exposed to H at 300 °C, 3D Ag clusters which had hexagonal shape and a flat top layer were obtained as a result of the disintegration of the 2D Ag layer into those clusters. The obtained result is similar to the H-induced self-organization processes in metal/Si systems.

II. EXPERIMENT

All experiments were carried out in an ultrahigh-vacuum (UHV) chamber with STM and low-energy electron diffraction (LEED) facilities. The base pressure in the UHV chamber was typically 8×10^{-11} Torr. The STM tip was fabricated by electrochemical etching from a tungsten wire (0.25 mm ϕ) and then cleaned by *in situ* annealing. An on-axis Si-terminated 6*H*-SiC crystal, commercially available from Cree Research (nitrogen doped, *n*-type, 0.062 Ωcm resistivity), was used in this study. The sample was cleaned by RCA procedure.[16] Then the sample was attached to the Mo sample holder and was placed in the UHV chamber. After outgassing at 650 °C for over 12 h, the $\sqrt{3}\times\sqrt{3}$ surface was prepared in the UHV chamber by exposing it to an Si flux at about 950 °C. Ag was evaporated from a tungsten basket coil by direct current heating. We controlled the amount of Ag deposition by means of a shutter set between the sample and the basket coil. The evaporation rate of Ag was about 0.04 monolayer (ML)/min [$1\ \mathrm{ML}=1.22\times10^{15}$ atoms/cm^2 on 6*H*-SiC(0001) plane]. For H exposure, H_2 gas was admitted into the chamber and dissociated into atomic H with an 1800 °C tungsten filament, 7 cm from the sample. Since the arrival rate of H is unknown, the dose of H_2 is expressed in units of langmuirs ($1\ \mathrm{L}=1\times10^{-6}$ Torr s). In our UHV system, to form a complete monohydride surface, a clean

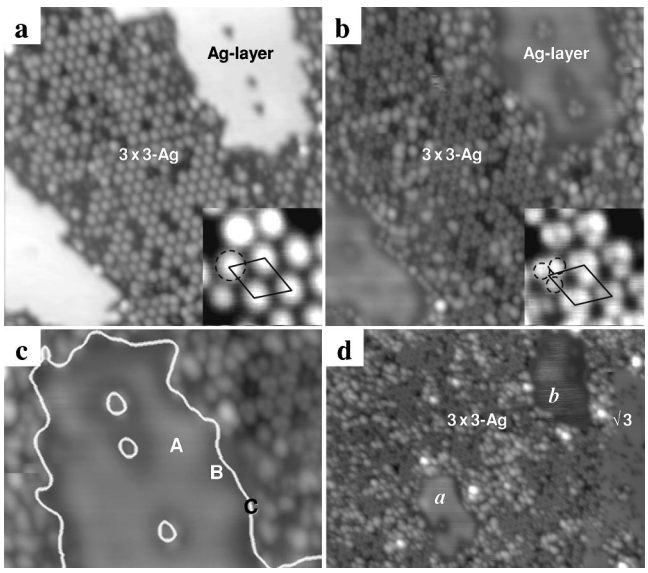

FIG. 1. (a) and (b) Dual-bias STM images (300×300 Å^2) of Ag/6*H*-SiC(0001) surface, which was formed by 0.2 ML Ag deposition onto a 6*H*-SiC(0001)$\sqrt{3}\times\sqrt{3}$ surface at 500 °C. The inset in each image shows the magnified image of Ag-induced 3×3 reconstruction (32×32 Å^2), in which a 3×3 unit cell is outlined. (c) The enlarged filled-state STM image of the Ag layer. The white line shows the profile of the borderline of Ag layer obtained from the empty-state image. (d) Two types of Ag layers: Ag layer surrounded by only 3×3 Ag and Ag layer surrounded by the 3×3-Ag (*a*) and $\sqrt{3}\times\sqrt{3}$ reconstructions (*b*). These images were taken under the following conditions: (a) $V_s=1.1$ V, $I_t=0.1$ nA; (b)–(d) $V_s=-1.1$ V, $I_t=0.1$ nA.

Si(100)2×1 surface must be exposed to 500 L H at 300 °C. All STM observations were carried out at room temperature (RT).

For a Si-terminated SiC(0001) surface, several surface reconstructions have been reported.[17–22] It has been established that a 3×3 surface phase can be reproducibly formed by annealing the sample at 800 °C in a flux of Si atoms supplied by an external source.[17,20] Upon further annealing, another surface phase, $\sqrt{3}\times\sqrt{3}$, is formed at 950 °C.[17–20] It has been established that the Si adatom model, which consists of 1/3 ML of Si adatoms in T_4 sites, is the most appropriate.[19,20]

III. RESULTS AND DISCUSSION

A. Ag/SiC surface phase

First, we formed a monatomic Ag layer on 6*H*-SiC(0001) substrate. Figures 1(a) and 1(b) show empty- and filled-state STM images of the surface prepared by nominal 0.2 ML Ag adsorption onto the $\sqrt{3}\times\sqrt{3}$ surface at 500 °C, respectively. In the empty-state image [Fig. 1(a)], a 3×3 periodic structure (referred to as 3×3-Ag hereafter) is observed, together with the original $\sqrt{3}\times\sqrt{3}$ surface. Moreover, a 2D homogeneous structure (referred to as Ag layer hereafter), in which some defects exist, is also observed with an apparent height of about 2 Å above the original $\sqrt{3}\times\sqrt{3}$ surface. The 3×3-Ag area and Ag layer coexisted up to the Ag coverage of 1 ML. The inset in Fig. 1(a) shows an enlarged empty-state STM image of the 3×3-Ag reconstruction. This reconstruction has a round protrusion per unit cell in the empty-state STM image with an apparent height of about 1 Å above the original $\sqrt{3}\times\sqrt{3}$ surface. In contrast, in the filled-state STM image, the 3×3-Ag reconstruction shows three small trimerlike protrusions per unit cell, which are nearly the same height as that on the $\sqrt{3}\times\sqrt{3}$ surface. It is well known that the 3×3 periodic structure is also formed as a clean surface on SiC(0001) substrate. However, the filled-state STM image of the clean SiC(0001)3×3 surface does not show such protrusions,[18] i.e., the structure of 3×3 Ag is different from that of the clean SiC(0001)3×3. On the other hand, the Ag layer exhibits a quite different morphology in the filled state. It appears to be an inhomogeneous layer as seen in Fig. 1(b), although no periodicity was observed on this structure in either the filled or empty state. Figure 1(c) shows the enlarged filled-state STM image of the Ag layer. The white line shows the profile of the borderline of the Ag layer obtained from the empty-state image. As can be seen, the area neighboring the borderline seems lower than the center part of the Ag layer, while there are some protrusions on the borderline. Figure 1(d) shows two types of Ag layers: the Ag layer surrounded by only the 3×3-Ag and the Ag layer surrounded by both the 3×3-Ag and $\sqrt{3}\times\sqrt{3}$ reconstructions. The height of the latter appears to be lower than that of the former in the filled state, while they appear to be almost the same height in the empty state (not shown here).

Let us discuss the structure of the Ag layer. When nominal 2 ML Ag atoms were deposited onto the $\sqrt{3}\times\sqrt{3}$ surface, most of the surface was covered by the Ag layer, and the LEED pattern showed 1×1 periodicity. Considering that an empty-state image of Ag layer was very flat as shown in Fig. 1(a), the atomic arrangement of Ag and Si (or C) atoms might be well ordered, i.e., they were arranged in a 1×1 periodicity rather than in disorder. In the topographic observation, however, the Ag layer did not show any periodicity at typical sample biases, as mentioned above. On this basis, it is suggested that most of Ag atoms incorporated in the Ag layer form metallic bonds with each other. Bearing in mind the Ag—Ag bond length in bulk (2.88 Å), it is also likely that the metallic Ag atoms in the Ag layer are arranged in a 1×1 periodicity with a 6*H*-SiC(0001) unit cell (3.08 Å).

Figure 2(a) shows STS spectra taken for the Ag-layer, 3×3-Ag, and $\sqrt{3}\times\sqrt{3}$ reconstructions, in which the current in each spectrum is extremely small below the Fermi level as compared with that above the Fermi level. Figure 2(b) shows optimized differential spectra $[(dI/dV)/(I/V)]$ of each spectrum shown in Fig. 2(a). As one can see, the density of state for the Ag layer does not show any band gap, which is consistent with the above consideration that the Ag layer exhibits metallic behavior, while that for $\sqrt{3}\times\sqrt{3}$ shows a large band gap, indicating semiconductorlike behavior. The 3×3-Ag surface shows a band gap closing as compared with the $\sqrt{3}\times\sqrt{3}$ surface. From this spectrum, however, it is difficult to determine whether the 3×3-Ag surface has metallic behavior or not. The spectrum for the Ag layer increases almost linearly above the Fermi level as shown in Fig. 2(a), while the increase is extremely small below the Fermi level

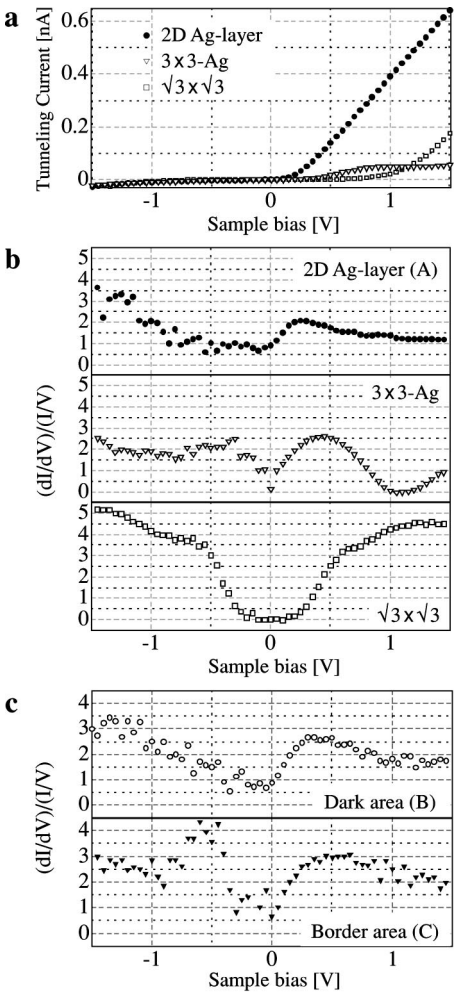

FIG. 2. (a) Scanning tunneling spectroscopy (STS) spectra taken for the 2D Ag-layer, 3×3-Ag, and $\sqrt{3}\times\sqrt{3}$ reconstructions. The initial set point of the spectra is $V_s=-1.2$ V, $I_t=0.013$ nA. (b) Optimized differential spectra of each spectrum shown in (a). (c) Optimized differential spectra taken for the locations indicated in Fig. 1(c); dark area (B) and border area (C) shown in filled state. The spectrum taken for bright area (A) is shown in (b) as a spectrum taken for a 2D Ag layer.

as occurs in the case of a diode. If this spectrum is dominated by the Schottky barrier at the interface between a 2D Ag layer and SiC bulk, the current should be small at a positive sample bias. Therefore, the Schottky barrier between Ag and SiC does not exist (or is not so large). One of the possible reasons for this phenomenon is explained by the spreading resistance and the band bending. In the case of an *n*-type substrate, the conduction band is near the Fermi level. It is well known that the band bending significantly occurs when the bias is applied between the tip and the SiC(0001)$\sqrt{3}\times\sqrt{3}$ surface, originating from a large spreading resistance from the tunneling point on the surface to the bulk.[23] However, in the case of the Ag layer, we postulate that the spreading resistance is small, since the surface electron transport easily occurs through the Ag layer, resulting in much of the current path from the surface to the bulk. This small spreading resistance of the 2D Ag layer might affect a large current flowing as compared with those of the $\sqrt{3}\times\sqrt{3}$ (and probably the 3×3-Ag). When the sample is negatively biased, the tunneling rate of electrons from the sample to the tip could be limited by the original carrier density in the bulk conduction band, since there is a large band gap below the Fermi level. As a result, the current was small as compared with that in the positive bias, in which the injected electrons from the tip could directly reach the bulk conduction band.

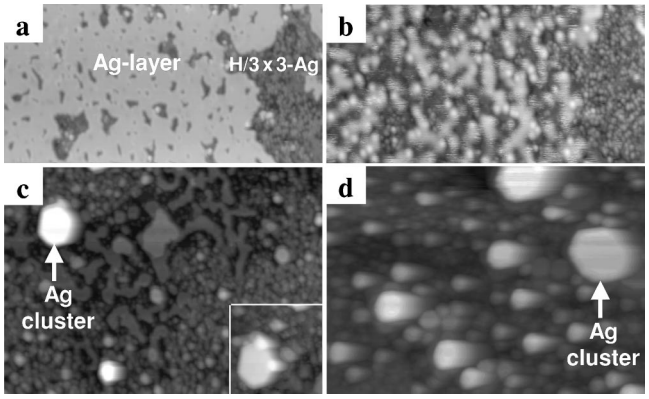

FIG. 3. A series of STM images [(a) and (b) 1000×500 Å^2; (c) and (d) 1000×720 Å^2] of Ag/6*H*-SiC(0001) $\sqrt{3}\times\sqrt{3}$ surface exposed to atomic H at 300 °C: (a) and (b) after exposure to 5 L of H; (c) after exposure to 30 L of H; (d) after exposure to 300 L of H. The images were taken under the following conditions; (a) $V_s=1.4$ V, $I_t=0.1$ nA; (b) $V_s=-1.4$ V, $I_t=0.1$ nA; (c) $V_s=2.6$ V, $I_t=0.1$ nA; (d) $V_s=1.6$ V, $I_t=0.1$ nA.

The filled-state image in the edge of the Ag layer seemed darker than that in the middle as mentioned in Fig. 1(c). The optimized differential spectra of other parts on the Ag layer are also shown in Fig. 2(c), which were taken at the locations indicated in Fig. 1(c); i.e., the dark area (B) and the border area (C). The spectrum taken on the bright area, indicated by A in Fig. 1(c), has previously shown in Fig. 2(b). One can see that no significant difference is seen between A and B. On the other hand, the spectrum for C exhibits a remarkable surface state at $E=-0.6$ eV. This indicates that the surface electronic structure of metallic bonds at the edge of the Ag layer would be perturbed by other surrounding reconstructions.

B. Hydrogen exposure of Ag/SiC

Next, the Ag/SiC(0001) surface obtained by nominal 1 ML Ag adsorption at 500 °C was exposed to H at 300 °C. Before H exposure, about 40% of the surface was covered by Ag-layer structures, while 40% was covered by the 3×3-Ag reconstructions. There also existed $\sqrt{3}\times\sqrt{3}$ reconstruction on this surface. Figure 3 shows a series of STM images of the Ag/SiC surface exposed to H. Upon H exposure, the 3×3-Ag area was immediately transformed into a disordered structure, and some defects were formed on the Ag layer, as shown in the empty-state image [Fig. 3(a)]. Moreover, the filled-state image shows many horizontal white lines [Fig. 3(b)]. It is likely that these noiselike lines

indicate the movements of Ag atoms, which may be induced by the electric field between the tip and the surface, i.e., the Ag layer appears to be unstable. With increasing H exposure, the defects on the Ag layer became larger, resulting in disintegration of more than 50% of the Ag layer after 30 L of H exposure [Fig. 3(c)]. At this stage, some hexagonal clusters were observed. A filled-state STM image of the cluster, indicated by an arrow, is also shown in the inset. These clusters exhibit a flat top surface in both filled- and empty-state images, which is different from the 2D Ag layer. The typical diameter and apparent height of the clusters were 50–100 Å and 14 Å, respectively. We postulate that these clusters are composed of Ag(111) monocrystallite, i.e., 2D Ag layer changes into 3D Ag clusters due to H exposure. Ag clusters were mainly formed on areas of the Ag layer, while the H-exposed 3×3-Ag area exhibited only a few Ag clusters. The Ag layer disappeared after exposure to 300 L of H as shown in Fig. 3(d). At this stage, the number of large Ag clusters was not much larger than that after exposure to 30 L of H, while the number of small Ag clusters (less than 50 Å in diameter) significantly increased. When the H-exposed surface was annealed at 500 °C, the surface reverted to the 3×3-Ag reconstruction and 2D Ag layer while no Ag cluster was observed. This result is similar to the morphological change of the Si(111)$\sqrt{3}\times\sqrt{3}$-Ag surface exposed to H.[13,24–26] According to the previous report,[24] H—Si bonds tend to be substituted for Ag—Si bonds when H atoms arrive onto the surface, since the H-terminated Si surface is more stable than the Ag/Si surface phase due to a larger bonding energy of H—Si than that of Ag—Si. Then, the expelled Ag atoms migrate on the surface, resulting in the formation of clusters. In addition, the $\sqrt{3}\times\sqrt{3}$-Ag surface is recovered after the desorption of H atoms at temperatures above 500 °C.

The schematic illustrations of H-induced cluster formation on 6*H*-SiC(0001) substrate are shown in Fig. 4. At he initial stage of H exposure, the 3×3-Ag area became disordered. The number of defects in the 2D Ag layer increased and each of them became larger [Fig. 4(b)], as Ag atoms in the Ag layer are driven out from the edges of the domain or defects. Upon further exposure, Ag islands are mainly formed on the 2D Ag layer [Fig. 4(c)]. This indicates that before H exposure most Ag atoms on the surface were incorporated into the 2D Ag layer rather than the 3×3-Ag area. At the initial stage of Ag cluster formation, large clusters tend to form, while at the final stage, large ones do not increase in size but small ones tend to increase in number [Fig. 4(d)]. Therefore, Ag atoms expelled by H atoms can easily migrate on the 2D Ag layer but can hardly move on the H-terminated SiC surface. Moreover, the 2D Ag-layer and 3×3-Ag areas were recovered by annealing the H-exposed surface, which implies the desorption of H atoms. Thus, the structural transformation process induced by H exposure is a common phenomenon between the Ag/6*H*-SiC(0001) and Ag/Si(111) surfaces. One may argue that such a 3D Ag cluster formation was caused by increasing the substrate temperature. However, no morphological change was observed when the original Ag/SiC surface was annealed at 500 °C without supplying H atoms. Thus, H atoms contribute to supply the expelled metal atoms. The elevation of the substrate temperature does not effect expelling of Ag atoms from the original position, but enhances the migration of Ag atoms expelled by H atoms.[14,27]

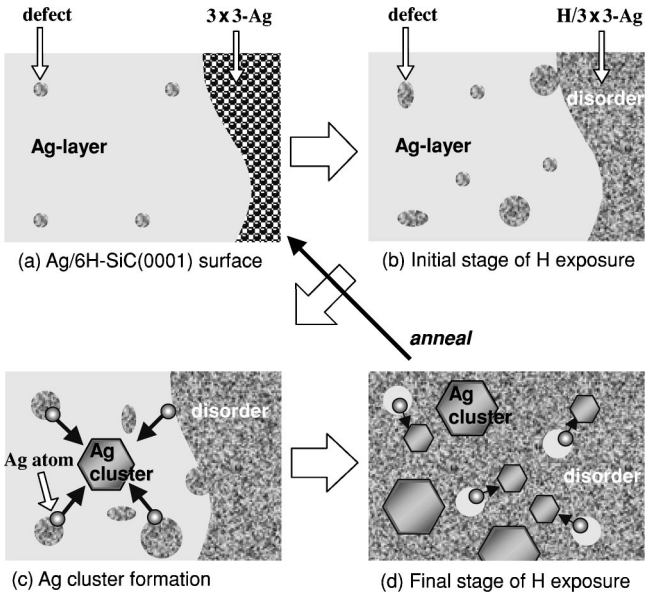

FIG. 4. Schematic illustrations of H-induced Ag cluster formation on 6*H*-SiC(0001) substrate. (a) Typical Ag/6*H*-SiC(0001) surface (before H exposure); (b)–(d): A series of illustrations showing the process of structural change on a Ag/6*H*-SiC(0001) surface induced by H exposure.

The apparent height of Ag clusters above the 2D Ag layer was 14 Å, while the monatomic height of Ag(111) monocrystallite is 2.34 Å. From these values, the thickness of Ag cluster is estimated to be about seven layers (additional six layers were formed on the original 2D Ag layer), although the heights in STM images do not always correspond to those of the actual atomic structures. Regarding the Si(111)$\sqrt{3}\times\sqrt{3}$-Ag exposed to H, the resultant Ag clusters are made up of about three or four layers.[24–26] There are two possible reasons for the cluster height difference between Ag/SiC(0001) and Ag/Si(111) systems. In regard to kinetics, it is likely that the surface diffusion length of Ag atoms on the Ag layer is larger than that of Ag atoms on the Si(111)$\sqrt{3}\times\sqrt{3}$-Ag domain. In regard to energetics, the difference between the interface energy between the substrate and Ag cluster (and the surface energy of Ag cluster) and the surface energy of H-terminated substrate for the Ag/SiC system is larger than that for the Ag/Si system.

IV. CONCLUSIONS

We observed surface phase formation in Ag/6*H*-SiC(0001) and its structural transformation process upon H exposure using scanning tunneling microscopy. A surface phase with 3×3 periodicity was found for Ag adsorption onto the $\sqrt{3}\times\sqrt{3}$ surface at 500 °C. On this surface,

we also observed the 2D Ag layer without showing any periodicities. The STS spectrum of the 2D Ag layer exhibited metallic behavior. When this surface was exposed to H at 300 °C, 3D Ag clusters which had hexagonal shape and a flat top layer were obtained as a result of the disintegration of the 2D Ag layer into those clusters. With increasing H exposure, the number of small Ag clusters increased, while that of large Ag clusters only slightly increased. The 3×3-Ag area and 2D Ag layer were reproduced by annealing at 500 °C. This result is similar to the H-induced cluster formation process on Si(111) substrates and demonstrates a deliberate formation of 3D metal dots on SiC surface.

ACKNOWLEDGMENTS

We would like to thank T. Harada and T. Kobayashi for their great help. This work was supported by a Grant-in-Aid for Scientific Research from the Ministry of Education, Culture, Sports, Science and Technology, Japan. One of the authors (O. K.) acknowledges the Japan Society for the Promotion of Science for providing a research fellowship.

*Present Address: Nanomaterials Laboratory, National Institute for Materials Science (NIMS), 1-2-1 Sengen, Tsukuba, Ibaraki 305-0047, Japan

†Corresponding author. Email address: katayama@ele.eng.osaka-u.ac.jp

[1] H. Morkoç, S. Strite, G. B. Gao, M. E. Lin, B. Sverdlov, and M. Burns, J. Appl. Phys. **76**, 1363 (1994).

[2] O. Kordina, J. P. Bergman, A. Henry, E. Janzén, S. Savage, J. André, L. P. Ramberg, U. Lindefelt, W. Hermansson, and K. Bergman, Appl. Phys. Lett. **67**, 1561 (1995).

[3] J. B. Casady and R. W. Johnson, Solid-State Electron. **39**, 1409 (1996).

[4] H. Yano, T. Hirao, T. Kimoto, and H. Matsunami, Appl. Phys. Lett. **78**, 374 (2001).

[5] T. Sakurai, M. Nishiyama, Y. Nishioka, and H. Kobayashi, Appl. Phys. Lett. **81**, 271 (2002).

[6] L.-Y. Chen, G. W. Hunter, P. G. Neudeck, G. Bansal, J. B. Petit, and D. Knight, J. Vac. Sci. Technol. A **15**, 1228 (1997).

[7] Q. Z. Xue, Q. K. Xue, R. Z. Bakhtizin, Y. Hasegawa, I. S. T. Tsong, T. Sakurai, and T. Ohno, Phys. Rev. B **59**, 12604 (1999).

[8] For example: V. Derycke, P. Fonteneau, N. P. Pham, and P. Soukiassian, Phys. Rev. B **63**, 201305 (2001).

[9] M. Hirai, Y. Marumoto, M. Kusaka, M. Iwami, T. Ozawa, T. Nagamura, and T. Nakata, Appl. Surf. Sci. **113/114**, 360 (1997).

[10] L. Li and I. S. T. Tsong, Surf. Sci. **364**, 54 (1996).

[11] For example: M. Katayama, R. S. Williams, M. Kato, E. Nomura, and M. Aono, Phys. Rev. Lett. **66**, 2762 (1991).

[12] K. Oura, V. G. Lifshits, A. A. Saranin, A. V. Zotov, and M. Katayama, Surf. Sci. Rep. **35**, 1 (1999) and references therein.

[13] K. Oura, H. Ohnishi, Y. Yamamoto, I. Katayama, and Y. Ohba, J. Vac. Sci. Technol. B **14**, 988 (1996).

[14] J. T. Ryu, T. Fuse, O. Kubo, T. Fujino, H. Tani, T. Harada, A. A. Saranin, A. V. Zotov, M. Katayama, and K. Oura, J. Vac. Sci. Technol. B **17**, 983 (1999).

[15] O. Kubo, T. Kobayashi, N. Yamaoka, A. A. Saranin, A. V. Zotov, H. Ohnishi, M. Katayama, and K. Oura, Phys. Rev. B **64**, 153406 (2001).

[16] W. Kern and D. A. Puotinen, RCA Rev. **31**, 187 (1970).

[17] F. Owman and P. Mårtensson, Surf. Sci. **330**, L639 (1995).

[18] L. Li and I. S. T. Tsong, Surf. Sci. **351**, 141 (1996).

[19] U. Starke, J. Schardt, J. Bernhardt, M. Franke, and K. Heinz, Phys. Rev. Lett. **82**, 2107 (1999).

[20] T. Fujino, T. Fuse, J.-T. Ryu, K. Inudzuka, Y. Yamazaki, M. Katayama, and K. Oura, Jpn. J. Appl. Phys. Part 1 **39**, 6410 (2000).

[21] U. Starke, J. Schardt, J. Bernhardt, M. Franke, K. Reuter, H. Wedler, K. Heinz, J. Furthmüller, P. Käckell, and F. Bechstedt, Phys. Rev. Lett. **80**, 758 (1998).

[22] M. Naitoh, J. Takami, S. Nishigaki, and N. Toyama, Appl. Phys. Lett. **75**, 650 (1999).

[23] V. Ramachandran and R. M. Feenstra, Phys. Rev. Lett. **82**, 1000 (1999).

[24] K. Oura, K. Sumitomo, T. Kobayashi, T. Kinoshita, Y. Tanaka, F. Shoji, and I. Katayama, Surf. Sci. **254**, L460 (1991).

[25] M. Aono, M. Katayama, and E. Nomura, Nucl. Instrum. Methods Phys. Res. B **64**, 29 (1992).

[26] H. Ohnishi, Y. Yamamoto, K. Oura, I. Katayama, and Y. Ohba, J. Vac. Sci. Technol. A **13**, 1438 (1995).

[27] J. T. Ryu, O. Kubo, T. Fujino, T. Fuse, T. Harada, K. Kawamoto, M. Katayama, A. A. Saranin, A. V. Zotov, and K. Oura, Surf. Sci. **447**, 117 (2000).